Multi-angle Imaging Spectro-Radiometer

Jet Propulsion Laboratory **Interoffice Memorandum**

MISR SCIENCE DFM #153

April 10, 1998

To: Carol Bruegge

From: Nadine C. Lu Chrien

Subject: BRF measurements made for MISR OBC

CC:

The MISR facility for the measurement of bidirectional reflectance properties is described in "Directional reflectance characterization facility and measurement methodology" (McGuckin, et al 1996). Presented here are the results from the final measurements taken to represent the MISR protoflight calibration panels (PF-4 and PF-5). The names of the data files collected to characterize the hemispheric BRF are listed in Table 1 and Table 2.

The MISR reflectance data consist of two measurements: the incident signal, V_i (referred to as "chan 1 out" in the data files), and the viewed (or reflectance) signal, V_v (referred to as "chan 0 out" in the data files). These measurements are taken for both s-polarization incident and p-polarization incident illumination conditions. These data are then converted to BRF. The BRF for an unpolarized source is then computed by taking the average of the s-polarization incident and p-polarization incident BRFs.

$$BRF(\theta_i;(\theta_r,\phi_r)) = \frac{V_v(\theta_i;(\theta_r,\phi_r))}{V_i(\mathrm{REF})}\cdot\frac{1}{C_{energy}\Omega_d 10^{\mathrm{ND}}}\cdot\frac{1}{\cos\theta_r} \quad (1)$$

$$C_{energy} = \frac{V_v(\text{energy calibration})}{V_i(\mathrm{REF})} \quad (2)$$

where,

Ω_d is the detector solid angle, 10^{ND} refers to the neutral density filter used in calibration, and C_{energy} is the mean value from the energy files taken for the data set.

Experimental Parameters

λ, nm	Ω_d, sr	10^{ND}
442	8.722e-4	3.126e3
632	8.722e-4	2.838e3
860	8.722e-4	4.074e3

The reflectance data were collected at 632.8 nm with source elevation angles of 8°, 40°, 45°, 50° and 55°. The source azimuth angle was at 0°. For each of these angles of incidence, the detector viewed the reflected signal at elevation angles, θ_r, of 1°, 10°, 20°, 30°, 40°, 50°, 60°, 70° and 80°. For each of these elevation angles, the detector viewed the reflected signal at azimuth angles, ϕ_r, from 0° to 180° at a sampling interval of 10°; symmetry in the BRF distribution for azimuth angles from 180° to 360° is assumed.

The measured BRF was resampled via spline interpolation/extrapolation and a numerical integration over the hemisphere was performed to arrive at the hemispheric reflectance factor (see Figure 1). The hemispheric reflectance factor (interpolated to 632 nm) measured by Labsphere for a source at 8° for the same sample was 0.983; a 0.8% difference from our result.

Table 1: Data files "Position 2" hemispheric, p-polarization incident

		θ_i [degrees]				
		8	40	45	50	55
calibration		97g08140.934	97g08162.728	97g14180.132	97g15123.751	97g22145.922
calibration		97g08141.015	97g08162.828	97g14180.216	97g15124.523	97g22150.011
θ_r [degrees]	1	97g08141.725	97g08163.501	97g14180.624	97g15124.909	97g22150.621
	10	97g08143.252	97g08164.605	97g14181.720	97g15130.313	97g22152.343
	20	97g08145.246	97g08170.004	97g14182.822	97g15131.455	97g22153.506
	30	97g08150.521	97g08171.047	97g14183.946	97g15132.547	97g22154.618
	40	97g08151.718	97g08172.400	97g14185.137	97g15133.959	97g22155.805
	50	97g08152.932	97g08173.730	97g14190.357	97g15135.151	97g22161.006
	60	97g08154.230	97g08175.010	97g14191.603	97g15140.844	97g22162.414
	70	97g08155.415	97g08180.425	97g14193.733	97g15142.511	97g22163.638
	80	97g08160.654	97g08181.634	97g14195.012	97g15143.717	97g22164.915
calibration		97g08162.515	97g08183.231	97g14200.502	97g15150.323	97g22170.419
calibration		97g08162.554	97g08183.339	97g14200.541	97g15150.401	97g22170.513
calibration		–	97g14134.319	–	–	–

Table 2: Data files "Position 2" hemispheric, s-polarization incident

		θ_i [degrees]				
		8	40	45	50	55
calibration		97g08111.810	97g14134.539	97g14160.014	97g15150.655	97g31145.102
calibration		97g08111.917	97g14134.639	97g14160.111	97g15150.746	97g31145.234
θ_r [degrees]	1	97g08112.716	97g14134.951	97g14160.613	97g15151.202	97g31145.614
	10	97g08113.855	97g14140.038	97g14161.802	97g15155.022	97g31150.739
	20	97g08123.115	97g14141.243	97g14162.838	97g15160.126	97g31152.040
	30	97g08124.245	97g14142.356	97g14163.935	97g15161.234	97g31153.130
	40	97g08125.608	97g14143.822	97g14165.249	97g15162.429	97g31154.229
	50	97g08131.003	97g14145.238	97g14170.607	97g15163.619	97g31155.508
	60	97g08132.305	97g14150.432	97g14171.906	97g15165.155	97g31160.646
	70	97g08133.637	97g14151.904	97g14173.242	97g15170.455	97g31162.312
	80	97g08135.112	97g14153.343	97g14174.440	97g15171.757	97g31164.553
calibration		97g08140.706	97g14155.130	97g14175.923	97g15173.531	97H31170.123
calibration		97g08140.809	97g14155.210	97g14180.000	97g15173.609	97H31170.209

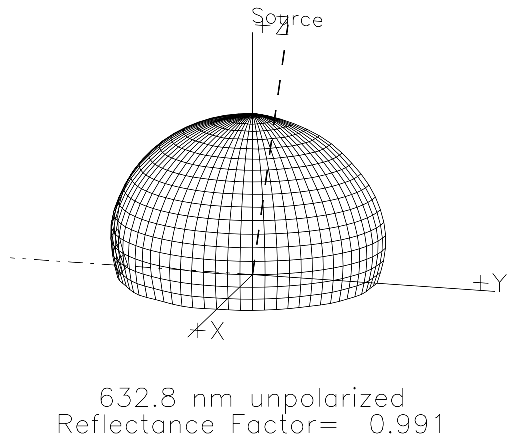

(a) θ_i= 8°

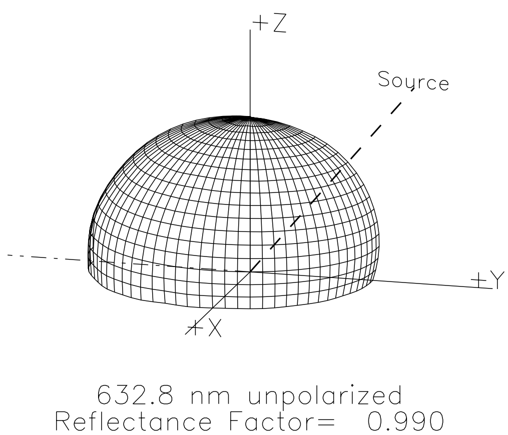

(b) θ_i= 40°

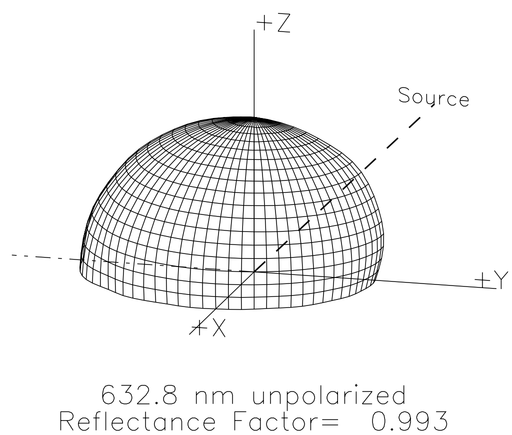

(c) θ_i= 45°

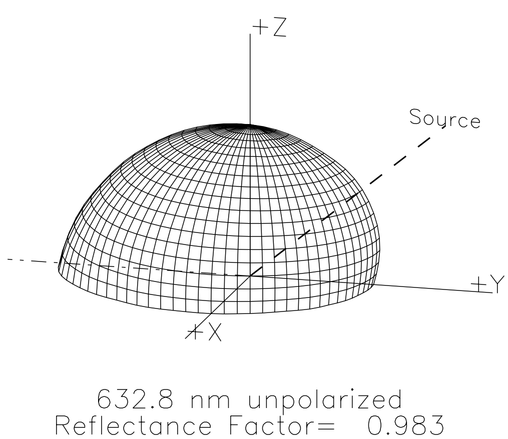

(d) θ_i= 50°

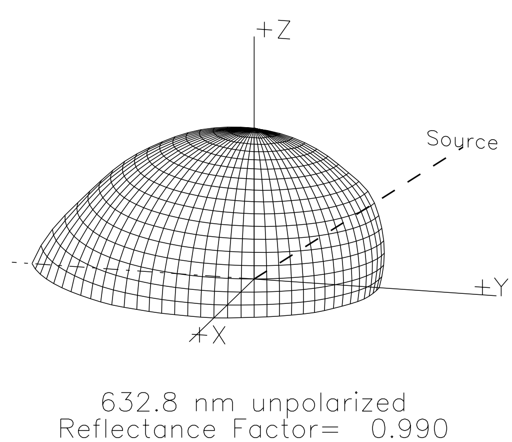

(e) θ_i= 55°

Figure 1. measured hemispheric BRF of test-piece 12669-2 to characterize PF calibration panels

The hemispheric measurements were performed on the test-piece as the laboratory setup did not allow such measurements to be done on the actual protoflight units. Only principal plane measurements could be done on the protoflight units. Figure 2 shows a comparison of the BRF in the principal plane (normalized to the BRF at $\theta_r = 0°$ as there were no calibration files done for the protoflight panels). It was discovered that the test-piece had two distinct regions to it. Rotation of the test-piece by 90° in the laboratory measurement setup did not affect the result. One region, referred to as "position 2" better matched the BRF results obtained from the protoflight units. The data from this position are the ones documented in this memorandum and which were provided as the "BRF database".

The protoflight panels, which are much longer than the test-piece did not exhibit this behavior when measured at various locations. It was subsequently noted by David Haner, who did the measurements, that there was a slight bump/dip in the test-piece in the vicinity of "position 1". It was barely noticeable and the anticipation was that the effect would be negligible. This was not however the case.

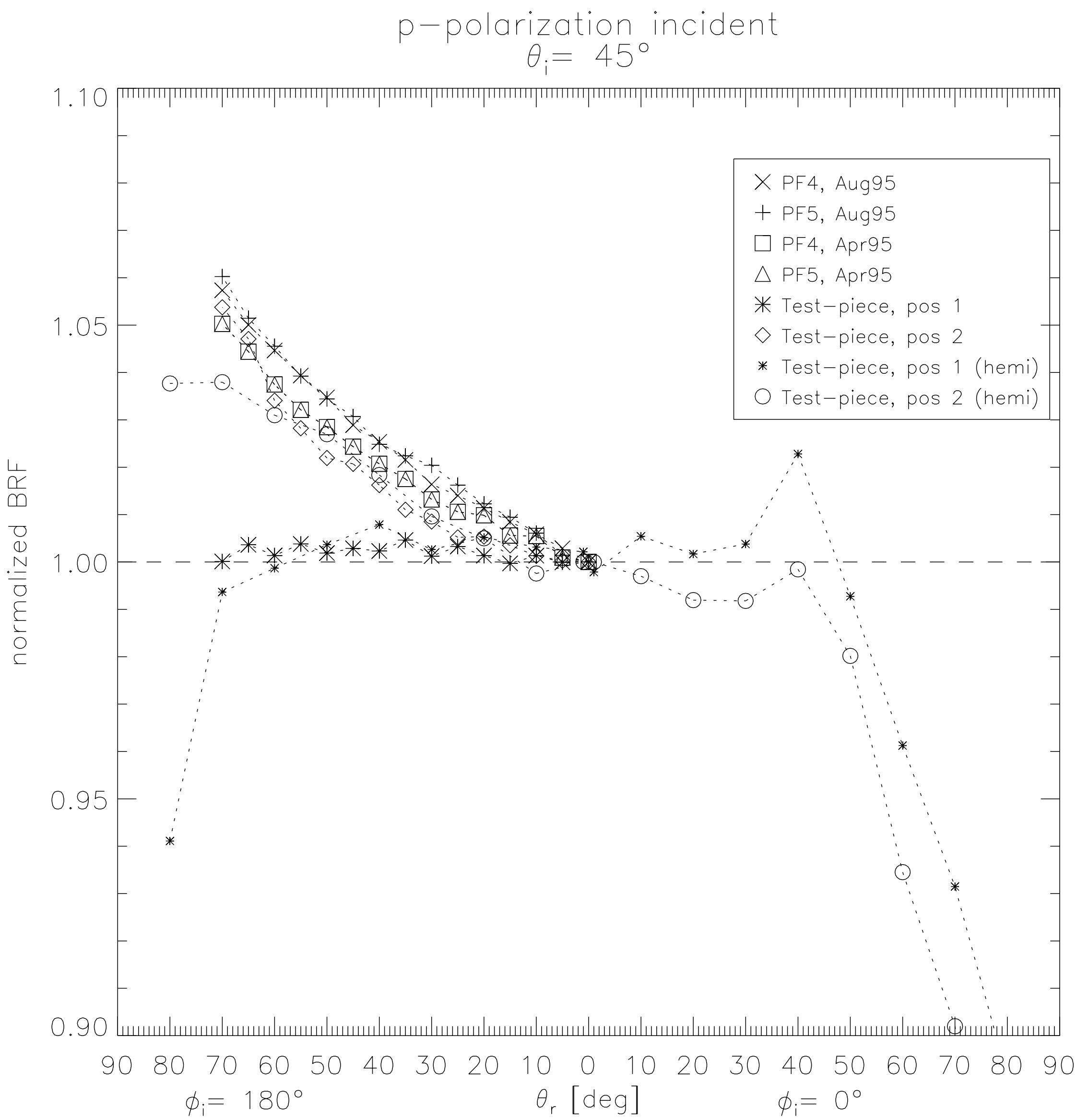

Figure 2. comparison of principal plane measurements on the protoflight panels with the test-piece

Figure 3 illustrates that the "position 2" data better characterize the MISR protoflight calibration panels. The expected range of view elevations from the MISR cameras is 9° to 70°. The anticipated solar incidence angle onto the calibration panels is from 38° to 55°.The azimuth angles relative to the source (which corresponds to our laboratory setup) will be on the ϕ_r = 180° side.

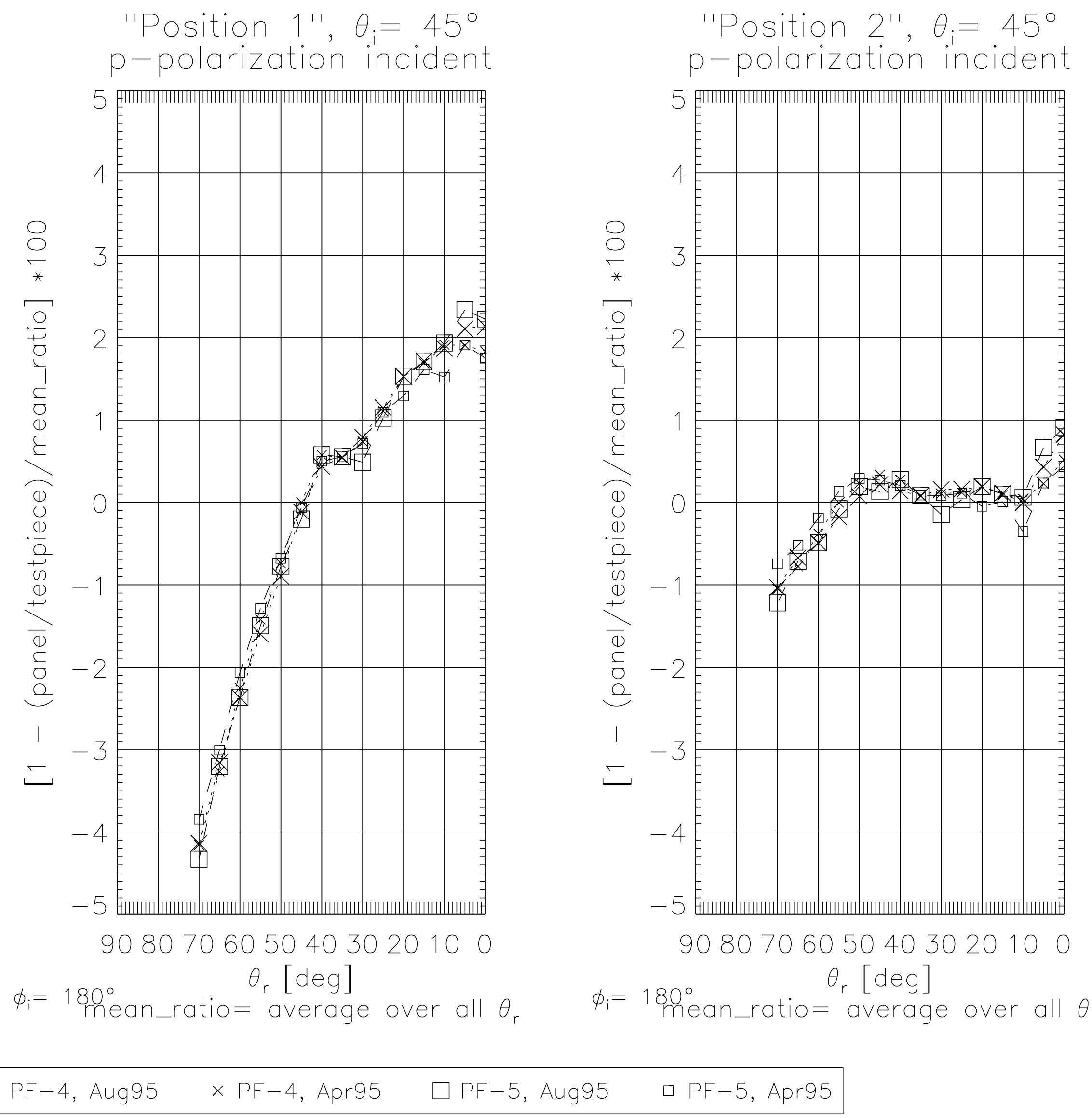

Figure 3. relative difference between protoflight panels and test-piece

The decision was made to acquire data for more illumination angles at a single wavelength (632 nm) rather than to acquire fewer illumination angles at all possible wavelengths (442 nm, 632 nm and 860 nm). The measurements that were done at 442 nm and 860 nm were made with the source at 55° and at "Position 1". In the interest of getting the best set of data to characterize the protoflight panels, subsequent testing, including the comparison of different locations on the test-piece were done at 632 nm only. Comparisons of the BRF with wavelength are shown in Figure 4 and Figure 5 and Table 3 and Table 4. The relative difference is less than 2.5%. As seen in Figure 2, the measurements for PF-4 and PF-5 vary by about 1% between Apr95 and Aug95. This could be due to slightly different locations on the panel having been measured or due to the realignment of the test setup. At any rate, the error due solely to wavelength difference is likely to be less than the 2.5% shown. Other contributing factors are the uncertainty in the calibration of the neutral density filter (see equation 1), the alignment of the test setup. The 442 nm laser and the 860 nm laser are not as easily aligned nor I believe quite as stable as the 632 nm laser.

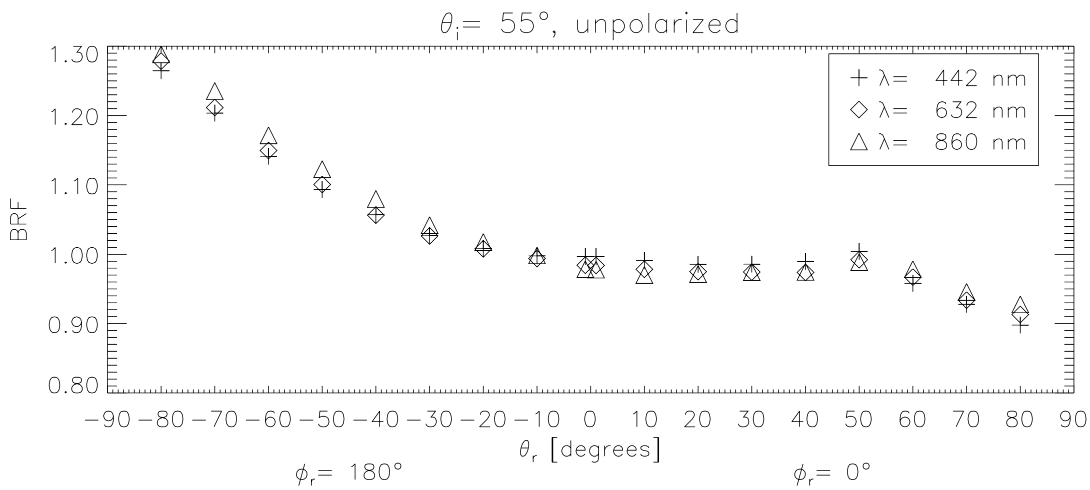

Figure 4. principal plane BRF with wavelength

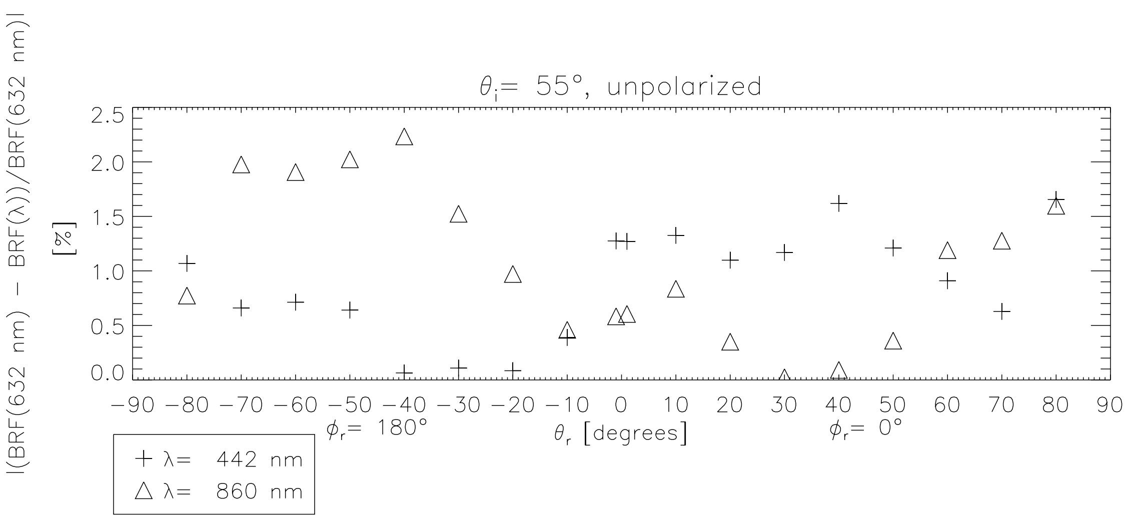

Figure 5. absolute percent difference in BRF from 632 nm

In conclusion, the BRF of the MISR protoflight calibration panels has been characterized. The assumption has been made that spectral variations in the BRF between the MISR wavelengths will be negligible when compared to other issues such as spatial variations on the protoflight panels themselves and the necessity of using the test-piece to characterize the BRF of the calibration panels, rather than doing a hemispheric BRF measurement on each of the protoflight panels directly.

Table 3: Percent difference between BRF measured at $\theta_i = 55°$ and 442 nm and 632.8 nm [%]

ϕ_r [deg]	θ_r [deg]								
	1.0	10.0	20.0	30.0	40.0	50.0	60.0	70.0	80.0
0.0	-1.3	-1.3	-1.1	-1.2	-1.6	-1.2	0.9	0.6	1.7
10.0	-1.3	-1.2	-1.0	-1.1	-1.5	-0.7	0.3	0.7	1.2
20.0	-1.3	-1.6	-1.1	-0.7	-1.0	-0.4	0.5	0.5	1.9
30.0	-1.3	-1.4	-1.0	-0.9	-0.9	-0.1	-0.1	0.1	1.5
40.0	-1.1	-1.0	-0.8	-0.9	-0.7	-0.2	0.1	-0.0	1.6
50.0	-1.2	-1.2	-0.7	-0.4	0.0	-0.0	0.2	0.6	0.7
60.0	-1.2	-1.5	-0.4	-0.4	-0.4	-0.2	0.1	0.0	1.1
70.0	-1.3	-1.2	-0.7	-0.3	-0.2	0.2	0.4	0.6	0.8
80.0	-1.2	-1.3	-0.4	-0.5	0.1	-0.1	0.2	0.5	1.3
90.0	-1.3	-1.4	-0.4	-0.3	-0.2	0.1	0.3	0.5	1.6
100.0	-1.0	-0.9	-0.3	-0.2	0.2	0.4	0.3	0.0	1.4
110.0	-1.2	-1.1	-0.2	0.2	0.0	0.3	0.6	0.3	1.1
120.0	-1.4	-0.8	-0.4	0.3	-0.1	0.5	0.2	1.0	0.6
130.0	-1.4	-0.7	-0.2	0.0	0.2	0.4	0.5	0.7	1.2
140.0	-1.5	-0.6	0.0	-0.1	0.3	0.5	0.9	0.7	0.7
151.0	-1.4	-0.1	-0.3	-0.1	0.7	0.6	1.2	0.8	1.0
160.0	-1.4	-0.7	-0.4	-0.2	0.0	0.8	0.8	0.8	1.7
170.0	-1.4	-0.5	-0.4	0.1	0.3	0.5	1.0	1.3	1.6
180.0	-1.3	-0.4	-0.1	-0.1	-0.1	0.6	0.7	0.7	1.1

Table 4: Percent difference between BRF measured at $\theta_i = 55°$ and 860 nm and 632.8 nm [%]

ϕ_r [deg]	θ_r [deg]								
	1.0	10.0	20.0	30.0	40.0	50.0	60.0	70.0	80.0
0.0	0.6	0.8	0.4	0.0	-0.1	0.4	-1.2	-1.3	-1.6
10.0	0.5	0.5	0.4	-0.2	-0.5	-1.0	-1.8	-1.2	-1.2
20.0	0.7	0.4	0.2	0.1	-0.8	-1.1	-0.6	-1.2	-1.4
30.0	0.7	0.2	-0.0	-0.2	-0.7	-1.1	-1.1	-0.8	-1.1
40.0	0.9	0.6	-0.2	-0.6	-0.8	-1.4	-1.3	-1.2	-0.5
50.0	0.8	0.2	-0.2	-0.6	-0.6	-1.2	-0.7	-0.3	-1.5
60.0	0.8	-0.2	-0.2	-0.8	-0.9	-1.3	-1.0	-1.1	-0.4
70.0	1.0	0.0	-0.6	-0.8	-0.9	-0.9	-0.7	-0.2	-0.4
80.0	1.0	-0.4	-0.4	-1.0	-1.1	-1.5	-1.1	-1.3	-0.9
90.0	0.8	0.0	-0.4	-0.8	-1.5	-1.0	-0.6	-1.2	0.1
100.0	0.6	-0.2	-0.3	-1.1	-1.1	-1.2	-1.1	-0.9	-0.3
110.0	0.6	-0.5	-0.4	-1.0	-1.7	-1.3	-1.0	-1.0	0.0
120.0	0.5	-0.4	-1.0	-0.9	-1.5	-1.4	-1.3	-0.5	-0.1
130.0	0.5	-0.3	-0.8	-1.4	-1.5	-1.4	-1.2	-1.5	-0.4
140.0	0.4	-0.1	-0.7	-1.3	-1.8	-1.7	-1.1	-1.7	-0.4
151.0	0.5	-0.4	-1.0	-1.4	-1.8	-1.3	-1.3	-1.8	-0.2
160.0	0.4	-0.5	-0.9	-1.5	-2.4	-2.1	-2.2	-2.1	-0.9
170.0	0.4	-0.1	-1.0	-1.4	-1.8	-1.6	-1.8	-2.1	-0.9
180.0	0.6	-0.5	-1.0	-1.5	-2.2	-2.0	-1.9	-2.0	-0.8